

Photochemical Synthesis of Pyrazolines from Tetrazoles in Flow

Adam Burke

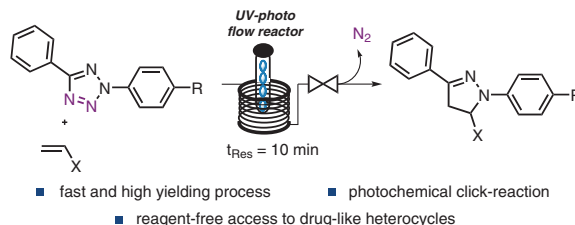
Silvia Spicchio

Mara Di Filippo

Marcus Baumann*

School of Chemistry, University College Dublin, Science Centre
South, D04 N2E2, Dublin, Ireland
marcus.baumann@ucd.ie

Published as part of the Virtual Collection
Click Chemistry and Drug Discovery



Received: 24.11.2022

Accepted after revision: 07.12.2022

Published online: 08.12.2022 (Accepted Manuscript),

22.02.2023 (Version of Record)

DOI: 10.1055/a-1995-1859; Art ID: SO-2022-11-0066-OP



License terms:

© 2022. The Author(s). This is an open access article published by Thieme under the terms of the Creative Commons Attribution License, permitting unrestricted use, distribution and reproduction, so long as the original work is properly cited.
(<https://creativecommons.org/licenses/by/4.0/>)

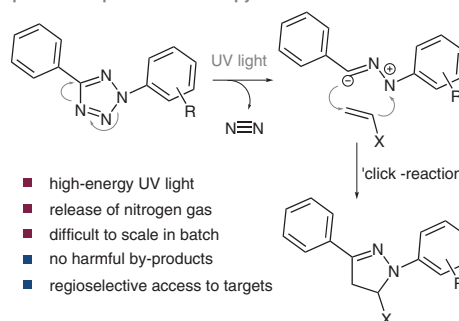
Abstract Pyrazolines and their pyrazole congeners are important heterocyclic building blocks with numerous applications in the fine chemical industries. However, traditional routes towards these entities are based on multistep syntheses generating substantial amounts of chemical waste. Here we report an alternative approach using UV-light to convert tetrazoles into pyrazolines via a reagent-free photo-click strategy. This route generates nitrile imine dipoles *in situ* that are trapped with different dipolarophiles rendering a selection of these heterocyclic targets in high chemical yields. A continuous flow method is ultimately realized that generates multigram quantities of product in a safe and readily scalable manner thus demonstrating the value of this photochemical approach for future exploitations in industry.

Key words flow chemistry, photochemistry, pyrazoline, tetrazole, click reaction, drug-like heterocycles

Pyrazolines are a class of pharmaceutically relevant five-membered heterocycles related to aromatic pyrazoles that possess myriad beneficial biological properties.¹ Together with their aromatic pyrazole counterparts, these scaffolds feature in numerous drugs, agrochemical agents, and their precursors.² Synthetically, pyrazolines are predominantly accessed through condensation reactions between hydrazines and enones or their derivatives.³ A different approach uses the dipolar cycloaddition between alkenes and *in situ* generated nitrile imines.⁴ Typically, nitrile imines are generated from α -halohydrazone in the presence of base,⁵ however, an alternative albeit underutilized entry to this dipole is available via the photolysis of tetrazoles.⁶ This option is potentially attractive as nitrogen gas is formed as the only by-product via a reagent-free re-

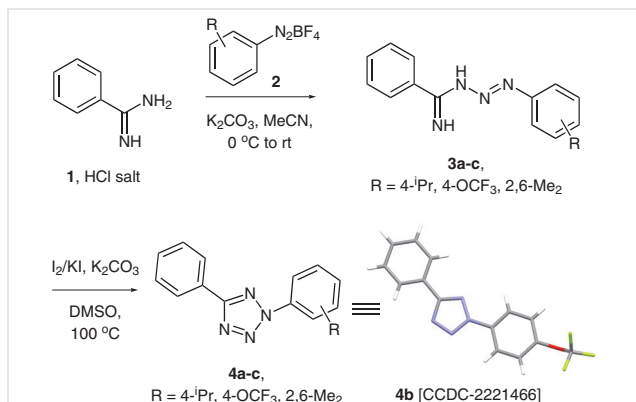
action that can be performed in the presence of the dipolarophile. As pyrazolines are continuing to be exploited in modern drug discovery programs improved protocols for their efficient and safe generation are in high demand. The adoption of continuous flow reactor technology has streamlined the synthesis of many fine chemical building blocks over the last few decades and provided for superior reactions through improved heat and mass transfer.^{7–10} More recently, this trend has witnessed the routine integration of photochemical reactions¹¹ to provide potentially more sustainable chemical syntheses.¹² Reactor miniaturization and high spatiotemporal control make continuous photochemical reactions a valuable tool to access a vast variety of chemical structures either facilitated by UV or visible light. Moreover, the uniform irradiation combined with short path lengths typical for flow photoreactors provides for good scalability of continuous photochemical processes.¹³ Due to these salient features, we wished to study the continuous photochemical generation of pyrazolines from tetrazole precursors to establish a safe and robust means for the generation of this important heterocyclic scaffold (Scheme 1).

photo-click process towards pyrazolines:



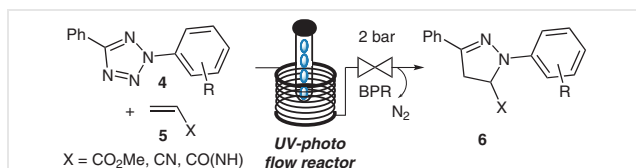
Scheme 1 Photochemical synthesis of pyrazolines from tetrazoles

To commence we prepared a small set of aryl-tetrazoles following literature-known protocols.¹⁴ The union of *in situ* generated arenediazonium salts **2** and benzamidine hydrochloride (**1**) thereby rendered the expected adducts **3a–c** in high yields which smoothly underwent oxidative cyclization to the desired tetrazole species **4**. The crystalline nature of tetrazole **4b** was exploited to perform single crystal diffraction studies¹⁵ and verify the anticipated connectivity of this heterocycle (Scheme 2).



Scheme 2 Synthesis of aryl-tetrazole substrates and X-ray crystallographic studies

Next, we embarked on developing a continuous flow approach for the photolysis of the tetrazole unit and the concomitant dipolar cycloaddition of the resulting nitrile imine with different dipolarophiles. We opted to use a standardized Vapourtec E-series flow reactor in combination with different light sources. Previous studies from our lab had identified both a medium-pressure Hg-lamp¹⁶ and a high-power UV-A LED (emitting at 365 nm)¹⁷ as valuable light sources in a number of related applications. Methyl methacrylate was chosen as model dipolarophile along with acetonitrile as reaction solvent. An adjustable back-pressure regulator (BPR) was set to 2 bar to control the release of stoichiometric amounts of nitrogen gas. The chosen set-up is depicted in Scheme 3 and allowed for quickly screening several variables such as reaction stoichiometry, concentration, and residence time.



Scheme 3 Flow photolysis set-up towards pyrazolines **6**

Initial experiments compared the UV-A LED (75 W input power) with the medium-pressure Hg-lamp (85 W input power) that was used in combination with a low-pass filter to exclude wavelengths above 400 nm. A stream of com-

pressed air was directed into the flow module to regulate the temperature to ca. 28 °C. Inside the reactor unit a tubular flow coil (10 mL, PFA) was fitted around the light source. The release of nitrogen gas bubbles after the BPR indicated photolytic cleavage of the tetrazole and formation of the anticipated pyrazoline **6** in case of the medium-pressure Hg-lamp. Interestingly, the UV-A LED did not generate the pyrazoline product (Table 1, entry 1) and the tetrazole substrate was recovered in almost quantitative yield indicating that light with wavelengths of 280–320 nm is critical for the photolysis step.¹⁸ Going forward, the medium-pressure Hg-lamp was further exploited in combination with the filter. As outlined in Table 1, substrate concentrations up to 100 mM were tolerated and only a small excess of the dipolarophile of 1.2 equiv. was needed. Degassing of the solvent did not provide any advantages indicating that residual oxygen is not detrimental under photochemical conditions. Furthermore, it was found that the residence time could be reduced from 20 min to 10 min, whereas shorter residence times of 5 min did not lead to full consumption of the tetrazole (entries 3–5). As expected, no product formed in the absence of UV-light (entry 6). Notably, the high concentration together with a short residence time of 10 minutes would provide for good reaction throughput in view of reaction scale-up.

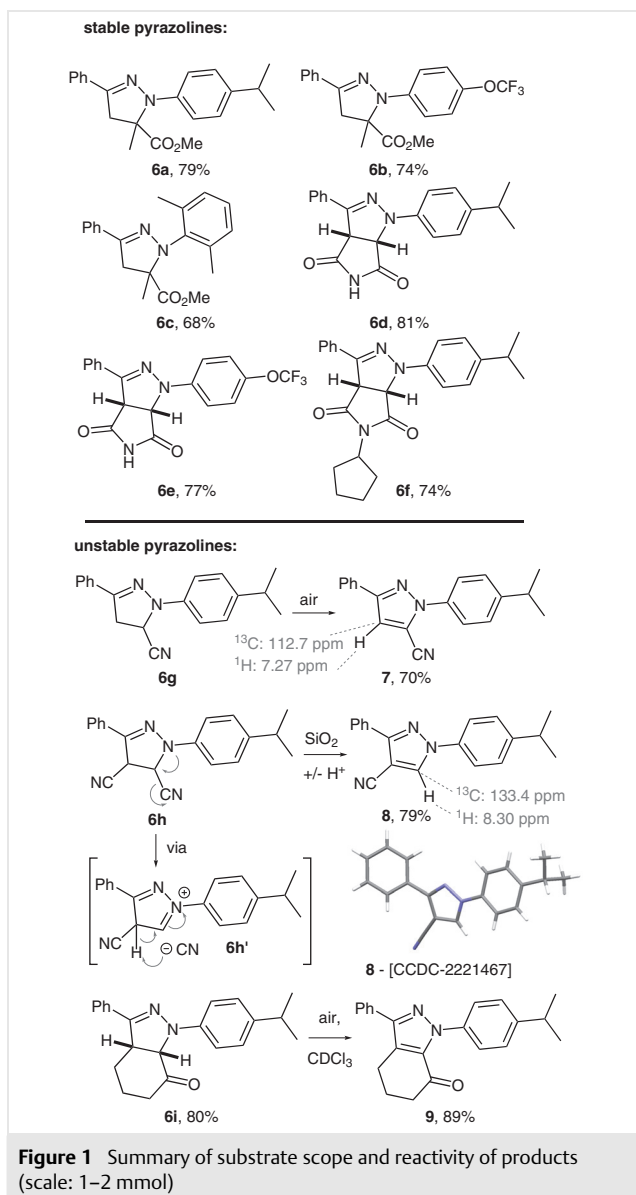
Table 1 Optimization Study for Model Pyrazoline Formation

Entry	Lamp	Conc. 4a (mM)	Equiv. 5	t_{Res} (min)	Yield (%)
1	365 nm LED	50	2.0	20	0
2	Hg-lamp ^a	50	2.0	20	65
3	Hg-lamp ^a	100	1.2	20	73
4	Hg-lamp ^a	100	1.2	10	79
5	Hg-lamp ^a	100	1.2	5	50 ^b
6	none	100	1.2	10	0

^a Filter used to exclude >400 nm light.

^b Ca. 45% of remaining substrate **4a**.

The optimized reaction conditions (Table 1, entry 4) were then applied to the preparation of pyrazolines **6a–c** and confirmed that all three tetrazoles underwent this tandem dipolar cycloaddition process smoothly (Figure 1). The desired pyrazolines were formed as single regioisomers in accordance with previous reports.⁴ Replacing methyl methacrylate with maleimide and *N*-cyclopentylmaleimide af-



forded the desired bicyclic pyrazolines **6d–f** in excellent yields. Next, acrylonitrile and fumaronitrile were trialed as alternative dipolarophiles. It was established that acrylonitrile forms the expected pyrazoline product **6g** in good yield (ca. 80% crude product by ^1H NMR), however, aerobic oxidation was found to be rapid yielding the nitrile-containing pyrazole product **7** after chromatographic purification. Similarly, fumaronitrile generated the anticipated dicyanopyrazoline **6h**, but after purification by silica gel chromatography the isomeric cyanopyrazole **8** was obtained as single regioisomer indicating elimination of HCN on contact with silica. Interestingly, these findings highlight a simple approach to access either of the regioisomeric forms **7** and

8 of these nitrile-substituted pyrazoles. Lastly, cyclohexenone was successfully used as dipolarophile together with tetrazole **4a** rendering the desired adduct **6i** in high yield after chromatographic purification. However, this compound underwent slow oxidation to the corresponding bicyclic pyrazole **9** in CDCl_3 , which could be suppressed by using $\text{DMSO}-d_6$ during NMR analysis.

A final part of this study concerned the scalability of the flow process in view of generating gram quantities of product. The reaction between tetrazole **4a** and maleimide under optimized conditions (Table 1, entry 4) was chosen for this test. A stock solution containing both reactants was prepared and processed through the photo-reactor under steady state conditions for a period of 2 h. Throughout this process formation of nitrogen gas was observed after the backpressure regulator indicating steady release of this gaseous by-product. The resulting product solution was concentrated under reduced pressure and subsequently cooled to 5 °C to initiate precipitation of the target product. After filtration and drying pyrazoline **6d** was obtained as a beige solid in 80% yield equating to a productivity of 1.6 g/h. Moreover, this material allowed for the generation of single crystals and verification of the anticipated connectivity of this product by means of single crystal X-ray diffraction.¹⁵ As depicted in Figure 2, the imide moiety thereby facilitates H-bonding between two molecules in the solid state.

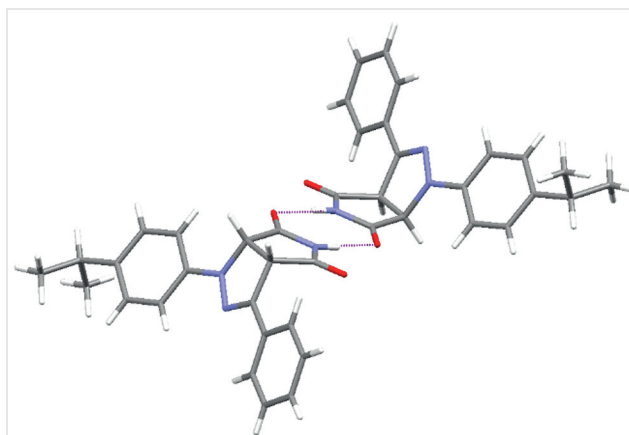


Figure 2 Crystal structure of **6d** displaying strong intermolecular H-bonding (CCDC-2221468)

In conclusion, we report a continuous photochemical click reaction converting arylated tetrazoles into various pyrazolines and pyrazoles. Using a medium-pressure Hg-lamp as light source combined with a low-pass filter to exclude wavelengths above 400 nm, these targets are generated in high yields (68–81%) in only 10 minutes residence time. The flow process is robust and tolerates concentrations of 100 mM which lends itself to generating gram quantities of products (throughput 6 mmol/h). The release of nitrogen gas that is formed along with the highly reactive

nitrile imine dipole is achieved safely and steadily using a backpressure regulator. Overall, this reagent-free flow process is attractive as it provides a sustainable entry to medicinally relevant pyrazoline building blocks and their pyrazole congeners in a highly efficient and scalable manner.

Solvents were purchased from Sigma-Aldrich and Fisher Scientific and used without further purification. Substrates and reagents were purchased from Alfa Aesar, Fisher Scientific, Fluorochem, or Sigma-Aldrich and used as received. ^1H NMR spectra were recorded with 400 and 500 MHz instruments and are reported relative to residual solvent: CHCl_3 ($\delta = 7.26$) and $\text{DMSO}-d_6$ ($\delta = 2.50$). ^{13}C NMR spectra were recorded with the same instruments (100 and 125 MHz) and again are reported relative to CHCl_3 ($\delta = 77.16$) and $\text{DMSO}-d_6$ ($\delta = 39.52$). COSY, HSQC, and HMBC, experiments were used in the structural assignment. IR spectra were recorded with a Bruker Platinum spectrophotometer (neat, ATR sampling) with the intensities of the characteristic signals being reported as weak (w, <20% of the tallest signal), medium (m, 21–70% of the tallest signal), or strong (s, >71% of the tallest signal). HRMS was performed using the indicated techniques with a micromass LCT orthogonal time-of-flight mass spectrometer with leucine-enkephalin (Tyr-Gly-Phe-Leu) as an internal lock mass. For UV/Vis measurements, a Shimadzu UV-1800 UV spectrophotometer was used. Continuous-flow experiments were performed with a Vapourtec E-Series system equipped with a UV150 photoreactor in combination with a high-power LED emitting light at 365 nm wavelength and a medium-pressure Hg-lamp (combined with a low-pass filter).

2,5-Diaryl-2H-tetrazoles 4a–c; General Procedure¹⁴

To a solution of concd HCl (3 mL, 12 M) at 0 °C was added the aniline (12 mmol) under stirring. After 5 min, a solution of NaNO_2 (12 mmol in 4 mL water) was added slowly and the suspension was stirred for a further 10 min before a solution of NaBF_4 (20 mmol in 4 mL water) was added. The mixture was stirred for 10 min and then the solid diazonium product **2** was isolated by filtration, washed with dilute NaBF_4 solution (ca. 5% w/w), and dried under suction.

To a suspension of benzamidine hydrochloride (**1**; 1 equiv., 0.4 M) and K_2CO_3 (3 equiv.) in MeCN/water (50:50) was added the diazonium tetrafluoroborate salt **2** (1 equiv.) at 0 °C. The mixture was stirred for 5 h at rt and then the aryl imino-triazine adduct **3** was isolated as a yellow solid by filtration, washed with water, and dried under suction.

A suspension of molecular I_2 (1.2 equiv.) and KI (1.5 equiv.) was prepared in DMSO (0.2 M) and stirred for 10 min at rt. Solid K_2CO_3 (3 equiv.) and the aryl imino-triazine adduct **3** (1 equiv.) were added and then the resulting mixture was heated to 100 °C for 1 h. After cooling to rt, the reaction mixture was quenched by addition of aq $\text{Na}_2\text{S}_2\text{O}_3$, followed by extractive workup with EtOAc and aqueous brine. Purification by chromatography (silica gel, EtOAc/cyclohexane 3:97) gave the tetrazole product **4** as a yellow oil or an off-white solid.

2-(4-Isopropylphenyl)-5-phenyl-2H-tetrazole (4a)

Yellow oil; yield: 3.4 g (12.8 mmol, 85%).

IR (neat): 2961 (m), 2870 (w), 1529 (m), 1511 (s), 1465 (s), 1449 (s), 1209 (s), 1052 (s), 835 (s), 729 (s), 689 cm^{-1} (s).

^1H NMR (CDCl_3 , 500 MHz): $\delta = 8.26$ (dd, $J = 8.0, 1.8$ Hz, 2 H), 8.10 (d, $J = 8.7$ Hz, 2 H), 7.54–7.49 (m, 3 H), 7.42 (d, $J = 8.4$ Hz, 2 H), 3.02 (hept, $J = 6.9$ Hz, 1 H), 1.31 (d, $J = 6.9$ Hz, 6 H).

^{13}C NMR (CDCl_3 , 125 MHz): $\delta = 165.0$ (C), 150.8 (C), 134.9 (C), 130.4 (CH), 128.9 (2 CH), 127.6 (2 CH), 127.3 (C), 127.0 (2 CH), 119.9 (2 CH), 33.9 (CH), 23.9 (2 CH_3).

HRMS (ESI+): m/z [$\text{M} + \text{H}$]⁺ calcd for $\text{C}_{16}\text{H}_{17}\text{N}_4$: 265.1448; found: 265.1446.

5-Phenyl-2-(4-(trifluoromethoxy)phenyl)-2H-tetrazole (4b)

Off-white solid; yield: 2.5 g (8.0 mmol, 80%).

IR (neat): 3077 (w), 1610 (w), 1531 (m), 1263 (s), 1208 (s), 1179 (s), 1015 (m), 856 (m), 726 (s), 683 cm^{-1} (s).

^1H NMR (CDCl_3 , 400 MHz): $\delta = 8.26$ –8.19 (m, 4 H), 7.52–7.46 (m, 3 H), 7.41 (d, $J = 8.0$ Hz, 2 H).

^{13}C NMR (CDCl_3 , 100 MHz): $\delta = 165.4$ (C), 149.6 (C), 135.1 (C), 130.7 (CH), 129.0 (2 CH), 127.0 (2 CH), 126.8 (C), 122.1, 121.3 (2 CH), 120.3 (q, $J = 257$ Hz, CF_3).

^{19}F NMR (CDCl_3 , 376 MHz): $\delta = -58.0$ (s).

HRMS (ESI+): m/z [$\text{M} + \text{H}$]⁺ calcd for $\text{C}_{14}\text{H}_{10}\text{N}_4\text{OF}_3$: 307.0801; found: 307.0802.

Crystal data (CCDC 2221466): $P2_1/n$; a 7.97598(18) Å, b 11.5500(2) Å, c 28.7873(7) Å, $\alpha = 90^\circ$, $\beta = 93.383(2)^\circ$, $\gamma = 90^\circ$.

2-(2,6-Dimethylphenyl)-5-phenyl-2H-tetrazole (4c)

Yellow oil; yield: 900 mg (3.6 mmol, 71%).

IR (neat): 3035 (w), 2926 (w), 1528 (m), 1465 (s), 1449 (s), 1362 (m), 1014 (s), 995 (m), 776 (s), 732 (s), 694 cm^{-1} (s).

^1H NMR ($\text{DMSO}-d_6$, 500 MHz): $\delta = 8.17$ –8.13 (m, 2 H), 7.61–7.56 (m, 3 H), 7.49 (t, $J = 7.7$ Hz, 1 H), 7.36 (d, $J = 7.7$ Hz, 2 H), 1.97 (s, 6 H).

^{13}C NMR ($\text{DMSO}-d_6$, 125 MHz): $\delta = 165.0$ (C), 136.1 (C), 135.4 (2 C), 131.6 (CH), 131.4 (CH), 129.8 (2 CH), 129.2 (2 CH), 127.1 (2 CH), 127.0 (C), 17.2 (2 CH_3).

HRMS (ESI+): m/z [$\text{M} + \text{H}$]⁺ calcd for $\text{C}_{15}\text{H}_{15}\text{N}_4$: 251.1291; found: 251.1292.

Pyrazolines 6a–f,i and Pyrazoles 7–9; General Procedure

A homogeneous solution containing tetrazole **4a–c** (1 equiv.) and dipolarophile **5** (1.2 equiv.) was prepared in MeCN (100 mM) and passed through the UV150 photoreactor of a Vapourtec E series system equipped with a medium-pressure Hg-lamp (85% input power, low-pass filter) and a flow coil (10 mL, PFA, residence time 10 min). Temperature control was provided via a stream of compressed air (ca. 28 °C internal reactor temperature). The exiting reaction mixture passed a BPR set to 2 bar before being collected in a flask. Evaporation of the solvent was followed by chromatography (silica gel, EtOAc/cyclohexane (10:90 to 20:80) to give the pyrazoline **6a–f,i** and pyrazole **7–9** after final evaporation of all volatiles.

Methyl 1-(4-Isopropylphenyl)-5-methyl-3-phenyl-4,5-dihydro-1H-pyrazole-5-carboxylate (6a)

Yellow oil; yield: 2.5 g (7.5 mmol, 79%).

IR (neat): 2956 (m), 2869 (w), 1735 (s), 1666 (w), 1610 (m), 1497 (s), 1447 (m), 1384 (s), 1257 (s), 1203 (s), 1121 (s), 1089 (s), 826 (s), 756 (s), 690 (s), 530 cm^{-1} (m).

^1H NMR (CDCl_3 , 500 MHz): $\delta = 7.73$ –7.69 (m, 2 H), 7.40 (dd, $J = 8.1, 6.6$ Hz, 2 H), 7.36–7.32 (m, 1 H), 7.14 (d, $J = 8.7$ Hz, 2 H), 7.06 (d, $J = 8.7$ Hz, 2 H), 3.78 (s, 3 H), 3.70 (d, $J = 16.6$ Hz, 1 H), 3.29 (d, $J = 16.6$ Hz, 1 H), 2.87 (hept, $J = 6.9$ Hz, 1 H), 1.64 (s, 3 H), 1.25 (d, $J = 6.9$ Hz, 6 H).

^{13}C NMR (CDCl_3 , 125 MHz): δ = 174.4 (C), 144.6 (C), 141.3 (C), 140.8 (C), 132.5 (C), 128.6 (2 CH + CH), 126.9 (2 CH), 125.6 (2 CH), 114.9 (2 CH), 69.2 (C), 52.9 (CH_3), 48.0 (CH_2), 33.3 (CH), 24.1 (2 CH_3), 21.0 (CH_3).

HRMS (ESI+): m/z [$\text{M} + \text{H}$] $^+$ calcd for $\text{C}_{21}\text{H}_{25}\text{N}_2\text{O}_2$: 337.1911; found: 337.1909.

Methyl 5-Methyl-3-phenyl-1-(4-(trifluoromethoxy)phenyl)-4,5-dihydro-1H-pyrazole-5-carboxylate (6b)

Yellow oil; yield: 1.4 g (3.7 mmol, 74%).

IR (neat): 2954 (w), 1739 (s), 1609 (w), 1509 (s), 1391 (w), 1253 (s), 1206 (s), 1162 (s), 1124 (m), 806 (w), 692 cm^{-1} (w).

^1H NMR (CDCl_3 , 400 MHz): δ = 7.71–7.66 (m, 2 H), 7.42–7.33 (m, 3 H), 7.05–7.14 (m, 4 H), 3.76 (s, 3 H), 3.71 (d, J = 16.8 Hz, 1 H), 3.30 (d, J = 16.8 Hz, 1 H), 1.64 (s, 3 H).

^{13}C NMR (CDCl_3 , 100 MHz): δ = 173.9 (C), 145.9 (C), 142.4 (C), 142.0 (C), 131.9 (C), 129.0 (CH), 128.6 (2 CH), 125.8 (2 CH), 122.0 (2 CH), 120.6 (CF_3 , q , J = 254 Hz), 115.1 (2 CH), 69.0 (C), 53.1 (CH_3), 48.3 (CH_2), 21.1 (CH_3).

^{19}F NMR (CDCl_3 , 376 MHz): δ = –58.3 (s).

HRMS (ESI+): m/z [$\text{M} + \text{H}$] $^+$ calcd for $\text{C}_{19}\text{H}_{18}\text{N}_2\text{O}_3\text{F}_3$: 379.1264; found: 379.1263.

Methyl 1-(2,6-Dimethylphenyl)-5-methyl-3-phenyl-4,5-dihydro-1H-pyrazole-5-carboxylate (6c)

Yellow oil; yield: 1.1 g (3.4 mmol, 68%).

IR (neat): 2950 (m), 1732 (s), 1586 (m), 1445 (s), 1365 (m), 1260 (m), 1201 (m), 1065 (m), 759 (s), 693 cm^{-1} (s).

^1H NMR (CDCl_3 , 400 MHz): δ = 7.67–7.63 (m, 2 H), 7.36 (dd, J = 8.3, 6.6 Hz, 2 H), 7.32–7.26 (m, 1 H), 7.03 (m, 3 H), 3.92 (d, J = 16.8 Hz, 1 H), 3.68 (s, 3 H), 3.19 (d, J = 16.8 Hz, 1 H), 2.19 (broad, 6 H)*, 1.42 (s, 3 H).

^{13}C NMR (CDCl_3 , 100 MHz): δ = 173.3 (C), 145.5 (C), 140.2 (C), 138.2 (2 C, broad)*, 132.9 (C), 129.1 (2 CH, broad)*, 128.5 (2 CH), 128.2 (CH), 127.1 (CH), 125.4 (2 CH), 70.9 (C), 52.4 (CH_3), 46.1 (CH_2), 22.1 (CH_3), 20.2 (CH_3)*, 18.7 (CH_3)*. The signals denoted with * appear broadened due to restricted rotation around the sterically congested C–N bond.

HRMS (ESI+): m/z [$\text{M} + \text{H}$] $^+$ calcd for $\text{C}_{20}\text{H}_{23}\text{N}_2\text{O}_2$: 323.1754; found: 323.1755.

1-(4-Isopropylphenyl)-3-phenyl-3a,6a-dihydropyrrolo[3,4-c]pyrazole-4,6(1H,5H)-dione (6d)

Yellow solid; yield: 3.2 g (9.6 mmol, 81%).

IR (neat): 3255 (broad), 2959 (m), 2869 (w), 1784 (s), 1610 (w), 1514 (s), 1381 (m), 1342 (m), 1207 (m), 1192 (m), 827 (m), 736 cm^{-1} (m).

^1H NMR (CDCl_3 , 400 MHz): δ = 8.43 (s, 1 H), 7.99 (d, J = 7.1 Hz, 2 H), 7.46 (d, J = 8.7 Hz, 1 H), 7.44–7.36 (m, 3 H), 7.20 (d, J = 8.6 Hz, 2 H), 5.11 (d, J = 10.9 Hz, 1 H), 4.85 (d, J = 10.9 Hz, 1 H), 2.87 (hept, J = 6.9 Hz, 1 H), 1.23 (d, J = 7.0 Hz, 6 H).

^{13}C NMR (CDCl_3 , 100 MHz): δ = 172.6 (C), 171.5 (C), 142.5 (C), 142.3 (C), 142.1 (C), 130.3 (C), 129.4 (CH), 128.6 (2 CH), 127.1 (2 CH), 127.0 (2 CH), 114.4 (2 CH), 66.9 (CH), 54.6 (CH), 33.4 (CH), 24.1 (CH_3), 24.1 (CH_3).

HRMS (ESI+): m/z [$\text{M} + \text{H}$] $^+$ calcd for $\text{C}_{20}\text{H}_{20}\text{N}_3\text{O}_2$: 334.1550; found: 334.1551.

Crystal data (CCDC-2221468): $P2_1/c$; a 17.3845(5) Å, b 6.2983(2) Å, c 15.8490(3) Å, α = 90°, β = 100.537(2)°, γ = 90°.

3-Phenyl-1-(4-(trifluoromethoxy)phenyl)-3a,6a-dihydropyrrolo[3,4-c]pyrazole-4,6(1H,5H)-dione (6e)

Beige solid; yield: 1.1 g (3.1 mmol, 77%).

IR (neat): 3203 (m), 3086 (w), 1774 (w), 1706 (s), 1508 (s), 1256 (s), 1200 (s), 1169 (s), 1090 (m), 1016 (m), 843 (m), 805 (m), 767 (m), 687 (m), 622 cm^{-1} (m).

^1H NMR ($\text{DMSO}-d_6$, 400 MHz): δ = 11.87 (br s, 1 H), 8.04–7.90 (m, 2 H), 7.52–7.46 (m, 2 H), 7.45–7.39 (m, 3 H), 7.31 (d, J = 8.7 Hz, 2 H), 5.33 (d, J = 10.7 Hz, 1 H), 5.13 (d, J = 10.7 Hz, 1 H).

^{13}C NMR ($\text{DMSO}-d_6$, 100 MHz): δ = 175.4 (C), 174.2 (C), 145.5 (C), 144.0 (C), 142.3 (C, q , J = 2 Hz), 130.8 (C), 129.9 (CH), 128.9 (2 CH), 127.5 (2 CH), 122.5 (2 CH), 120.7 (CF_3 , q , J = 254 Hz), 115.2 (2 CH), 67.0 (CH), 55.6 (CH).

^{19}F NMR ($\text{DMSO}-d_6$, 376 MHz): δ = –57.2 (s).

HRMS (ESI+): m/z [$\text{M} + \text{H}$] $^+$ calcd for $\text{C}_{18}\text{H}_{13}\text{N}_3\text{O}_3\text{F}_3$: 376.0904; found: 376.0903.

5-Cyclopentyl-1-(4-isopropylphenyl)-3-phenyl-3a,6a-dihydropyrrolo[3,4-c]pyrazole-4,6(1H,5H)-dione (6f)

Beige solid; yield: 1.2 g (2.9 mmol, 74%).

IR (neat): 2957 (m), 2870 (w), 1703 (s), 1610 (m), 1513 (s), 1446 (w), 1369 (s), 1220 (m), 1158 (m), 891 (m), 735 (s), 690 cm^{-1} (s).

^1H NMR (CDCl_3 , 400 MHz): δ = 8.05 (d, J = 7.0 Hz, 2 H), 7.52 (d, J = 8.8 Hz, 2 H), 7.47–7.33 (m, 3 H), 7.21 (d, J = 8.8 Hz, 2 H), 5.08 (d, J = 11.0 Hz, 1 H), 4.80 (d, J = 11.0 Hz, 1 H), 4.48 (p, J = 8.3 Hz, 1 H), 2.88 (hept, J = 6.9 Hz, 1 H), 2.01–1.78 (m, 6 H), 1.59–1.54 (m, 2 H), 1.23 (d, J = 7.0 Hz, 6 H).

^{13}C NMR (CDCl_3 , 100 MHz): δ = 172.8 (C), 171.9 (C), 142.7 (C), 142.4 (C), 142.0 (C), 130.6 (C), 129.3 (CH), 128.5 (2 CH), 127.1 (2 CH), 127.0 (2 CH), 114.4 (2 CH), 65.5 (CH), 53.2 (CH), 52.5 (CH), 33.4 (CH), 28.8 (CH_2), 28.7 (CH_2), 25.3 (CH_2), 25.3 (CH_2), 24.1 (CH_3), 24.1 (CH_3).

HRMS (ESI+): m/z [$\text{M} + \text{H}$] $^+$ calcd for $\text{C}_{25}\text{H}_{28}\text{N}_3\text{O}_2$: 402.2176; found: 402.2176.

1-(4-Isopropylphenyl)-3-phenyl-1,3a,4,5,6,7a-hexahydro-7H-indazol-7-one (6i)

Yellow waxy solid; yield: 700 mg (2.1 mmol, 80%).

IR (neat): 2956 (m), 2866 (w), 1716 (s), 1610 (m), 1514 (s), 1378 (m), 1123 (m), 828 (m), 766 (m), 693 cm^{-1} (m).

^1H NMR ($\text{DMSO}-d_6$, 400 MHz): δ = 7.74–7.70 (m, 2 H), 7.45–7.33 (m, 3 H), 7.09 (d, J = 8.6 Hz, 2 H), 6.99 (d, J = 8.7 Hz, 2 H), 4.50 (d, J = 11.3 Hz, 1 H), 4.38 (dt, J = 11.4, 6.0 Hz, 1 H), 2.77 (h, J = 6.9 Hz, 1 H), 2.44–2.33 (m, 2 H), 1.94–1.78 (m, 3 H), 1.57–1.47 (m, 1 H), 1.14 (d, J = 6.9 Hz, 6 H).

^{13}C NMR ($\text{DMSO}-d_6$, 100 MHz): δ = 209.9 (C), 152.3 (C), 144.6 (C), 140.6 (C), 131.2 (C), 129.4 (CH), 129.2 (2 CH), 127.1 (2 CH), 126.6 (2 CH), 114.5 (2 CH), 70.2 (CH), 49.3 (CH), 37.8 (CH_2), 33.1 (CH), 24.9 (CH_2), 24.5 (2 CH_3), 21.0 (CH_2).

HRMS (ESI+): m/z [$\text{M} + \text{H}$] $^+$ calcd for $\text{C}_{22}\text{H}_{25}\text{N}_2\text{O}$: 333.1961; found: 333.1961.

1-(4-Isopropylphenyl)-3-phenyl-1H-pyrazole-5-carbonitrile (7)

Yellow oil; yield: 500 mg (1.8 mmol, 70%).

IR (neat): 3048 (s), 2961 (m), 2927 (w), 2235 (m), 1515 (s), 1459 (m), 1434 (m), 1357 (m), 837 (s), 767 (s), 693 cm^{-1} (s).

^1H NMR (CDCl_3 , 400 MHz): δ = 7.86–7.83 (m, 2 H), 7.67 (d, J = 8.5 Hz, 2 H), 7.44 (dd, J = 8.2, 6.4 Hz, 2 H), 7.41–7.36 (m, 3 H), 7.27 (s, 1 H), 2.99 (hept, J = 7.3 Hz, 1 H), 1.29 (d, J = 7.0 Hz, 6 H).

^{13}C NMR (CDCl_3 , 100 MHz): δ = 152.5 (C), 150.0 (C), 136.4 (C), 131.2 (C), 128.9 (CH), 128.9 (2 CH), 127.5 (2 CH), 125.9 (2 CH), 122.9 (2 CH), 114.9 (C), 112.7 (CH), 111.2 (C), 33.9 (CH), 23.9 (2 CH_3).

HRMS (ESI⁺): m/z [$\text{M} + \text{H}$]⁺ calcd for $\text{C}_{19}\text{H}_{18}\text{N}_3$: 288.1495; found: 288.1496.

1-(4-Isopropylphenyl)-3-phenyl-1H-pyrazole-4-carbonitrile (8)

Pale yellow solid; yield: 905 mg (3.2 mmol, 79%).

IR (neat): 3130 (w), 2960 (s), 2928 (w), 2226 (m), 1534 (s), 1515 (m), 1450 (m), 1360 (m), 1229 (m), 1054 (m), 960 (m), 831 (m), 774 (m), 695 cm^{-1} (m).

^1H NMR (CDCl_3 , 400 MHz): δ = 8.30 (s, 1 H), 8.06 (dd, J = 8.4, 1.4 Hz, 2 H), 7.63 (d, J = 8.5 Hz, 2 H), 7.51–7.41 (m, 3 H), 7.35 (d, J = 8.5 Hz, 2 H), 2.97 (hept, J = 6.9 Hz, 1 H), 1.28 (d, J = 7.0 Hz, 6 H).

^{13}C NMR (CDCl_3 , 100 MHz): δ = 153.7 (C), 149.3 (C), 136.7 (C), 133.4 (CH), 130.5 (C), 129.5 (CH), 128.9 (2 CH), 127.7 (2 CH), 126.8 (2 CH), 119.8 (2 CH), 114.3 (C), 91.4 (C), 33.8 (CH), 23.9 (2 CH_3).

HRMS (ESI⁺): m/z [$\text{M} + \text{H}$]⁺ calcd for $\text{C}_{19}\text{H}_{18}\text{N}_3$: 288.1495; found: 288.1494.

Crystal data (CCDC-2221467): $P1$; a 9.0051(2) Å, b 11.4268(2) Å, c 15.6532(3) Å, α = 94.185(2)°, β = 98.826(2)°, γ = 106.996(2)°.

1-(4-Isopropylphenyl)-3-phenyl-1,4,5,6-tetrahydro-7H-indazol-7-one (9)

Yellow solid; yield: 725 mg (2.2 mmol, 89%).

IR (neat): 2957 (m), 2869 (w), 1685 (s), 1515 (m), 1435 (m), 1015 (m), 919 (m), 836 (m), 696 (m), 550 cm^{-1} (m).

^1H NMR (CDCl_3 , 500 MHz): δ = 7.79 (dd, J = 7.6, 1.6 Hz, 2 H), 7.50–7.44 (m, 4 H), 7.41–7.36 (m, 1 H), 7.32 (d, J = 8.5 Hz, 2 H), 3.06 (t, J = 6.1 Hz, 2 H), 2.99 (hept, J = 6.9 Hz, 1 H), 2.64 (dd, J = 7.3, 5.5 Hz, 2 H), 2.22 (p, J = 6.2 Hz, 2 H), 1.30 (d, J = 6.9 Hz, 6 H).

^{13}C NMR (CDCl_3 , 125 MHz): δ = 188.3 (C), 149.0 (C), 148.6 (C), 137.9 (C), 135.7 (C), 132.6 (C), 128.7 (2 CH), 128.6 (C), 128.1 (CH), 127.2 (2 CH), 126.5 (2 CH), 125.3 (2 CH), 39.7 (CH_2), 33.9 (CH), 24.7 (CH_2), 23.9 (2 CH_3), 22.8 (CH_2).

HRMS (ESI⁺): m/z [$\text{M} + \text{H}$]⁺ calcd for $\text{C}_{22}\text{H}_{23}\text{N}_2\text{O}$: 331.1805; found: 331.1812.

Conflict of Interest

The authors declare no conflict of interest.

Funding Information

This research was supported by Science Foundation Ireland (12/RC2275_P2 and 18/RI/5702), the Royal Society of Chemistry (Research Enablement Grant; E20-2998), and the School of Chemistry through provision of a Sir Walter Hartley scholarship to M.D.F.

Acknowledgment

We grateful to Dr Julia Bruno and Dr Andrew D. Phillips for solving the crystal structures reported in this paper as well as Dr Jimmy Muldoon and Dr Yannick Ortin for assistance with MS and NMR experiments.

Supporting Information

Supporting information for this article is available online at <https://doi.org/10.1055/a-1995-1859>.

References

- (1) (a) Ahsan, M. J.; Ali, A.; Ali, A.; Thiriveedhi, A.; Bakht, M. A.; Yusuf, M.; Salahuddin; Afzal, O.; Altamimi, A. S. A. *ACS Omega* **2022**, 7, 38207. (b) Haider, K.; Shafeeqe, M.; Yahya, S.; Yar, M. S. *Eur. J. Med. Chem. Rep.* **2022**, 5, 100042. (c) Kumari, P.; Mishra, V. S.; Narayana, C.; Khanna, A.; Chakrabarty, A.; Sagar, R. *Sci. Rep.* **2020**, 10, 6660.
- (2) (a) Baumann, M.; Baxendale, I. R.; Ley, S. V.; Nikbin, N. *Beilstein J. Org. Chem.* **2011**, 7, 442. (b) Silver, K. S.; Soderlund, D. M. *Pestic. Biochem. Physiol.* **2005**, 82, 136. (c) Mertens, L.; Hock, K. J.; Koenigs, R. M. *Chem. Eur. J.* **2016**, 22, 9542. (d) Alex, K.; Tillack, A.; Schwarz, N.; Beller, M. *Org. Lett.* **2008**, 10, 2377.
- (3) (a) Vahedpour, T.; Hamzeh-Mivehroud, M.; Hemmati, S.; Dastmalchi, S. *ChemistrySelect* **2021**, 6, 6483. (b) Lévai, A. *Chem. Heterocycl. Compd.* **1997**, 33, 647. (c) Li, Y.; Wei, L.; Wan, J.-P.; Wen, C. *Tetrahedron* **2017**, 73, 2323. (d) Golovanov, A. A.; Odin, I. S.; Gusev, D. M.; Vologzhanina, A. V.; Sosnin, I. M.; Grabovskiy, S. A. *J. Org. Chem.* **2021**, 86, 7229.
- (4) (a) Bégué, D.; Dargelos, A.; Wentrup, C. *J. Org. Chem.* **2020**, 85, 7952. (b) Bégué, D.; Qiao, G. G.; Wentrup, C. *J. Am. Chem. Soc.* **2012**, 134, 5339. (c) Nunes, C. M.; Reva, I.; Fausto, R.; Bégué, D.; Wentrup, C. *Chem. Commun.* **2015**, 51, 14712. (d) Deepthi, A.; Acharjee, N.; Sruthi, S. L.; Meenakshy, C. B. *Tetrahedron* **2022**, 116, 132812.
- (5) (a) Wang, Y.-G.; Zhang, J.; Lin, X.-F.; Ding, H.-F. *Synlett* **2003**, 1467. (b) Alizadeh, A.; Moafi, L.; Zhu, L.-G. *Synlett* **2016**, 27, 595. (c) Utecht, G.; Fruziński, A.; Jasiński, M. *Org. Biomol. Chem.* **2018**, 16, 1252.
- (6) (a) Wang, Y.; Rivera Vera, C. I.; Lin, Q. *Org. Lett.* **2007**, 9, 4155. (b) Clovis, J. S.; Eckell, A.; Huisgen, R.; Sustmann, R. *Chem. Ber.* **1967**, 100, 60. (c) Padwa, A.; Nahm, S.; Sato, E. *J. Org. Chem.* **1978**, 43, 1664.
- (7) (a) Plutschack, M. B.; Pieber, B.; Gilmore, K.; Seeberger, P. H. *Chem. Rev.* **2017**, 117, 11796. (b) Gutmann, B.; Cantillo, D.; Kappe, C. O. *Angew. Chem. Int. Ed.* **2015**, 54, 6688. (c) Colella, M.; Nagaki, A.; Luisi, R. *Chem. Eur. J.* **2020**, 26, 19.
- (8) (a) Dallinger, D.; Gutmann, B.; Kappe, C. O. *Acc. Chem. Res.* **2020**, 53, 1330. (b) Movsisyan, M.; Delbeke, E. I. P.; Berton, J. K. E. T.; Battilocchio, C.; Ley, S. V.; Stevens, C. V. *Chem. Soc. Rev.* **2016**, 45, 4892.
- (9) (a) Fitzpatrick, D. E.; Ley, S. V. *Tetrahedron* **2018**, 74, 3087. (b) Adamo, A.; Beingessner, R. L.; Behnam, M.; Chen, J.; Jamison, T. J.; Jensen, K. F.; Monbaliu, J.-C. M.; Myerson, A. S.; Revalor, E. M.; Snead, D. R.; Stelzer, T.; Weeranoppanant, N.; Wong, S. Y.; Zhang, P. *Science* **2016**, 352, 61.
- (10) (a) Breen, C. P.; Nambiar, A. M. K.; Jamison, T. F.; Jensen, K. F. *Trends Chem.* **2021**, 3, 373. (b) Gioiello, A.; Piccinno, A.; Lozza, A. M.; Cerra, B. *J. Med. Chem.* **2020**, 63, 6624. (c) Baumann, M.;

- Moody, T. S.; Smyth, M.; Wharry, S. *Org. Process Res. Dev.* **2020**, *24*, 1802. (d) Baxendale, I. R.; Brocken, L.; Mallia, C. J. *Green Process Synth.* **2013**, *2*, 211.
- (11) (a) Buglioni, L.; Raymenants, F.; Slattery, A.; Zondag, S. D. A.; Noël, T. *Chem. Rev.* **2022**, *122*, 2752. (b) Samiango, C.; Noël, T. *Trends Chem.* **2020**, *2*, 92. (c) Elliott, L. D.; Knowles, J. P.; Koovits, P. J.; Maskil, K. G.; Ralph, M. J.; Lejeune, G.; Edwards, L. J.; Robinson, R. I.; Clemens, I. R.; Cox, B.; Pascoe, D. D.; Koch, G.; Eberle, M.; Berry, M. B.; Booker-Milburn, K. I. *Chem. Eur. J.* **2014**, *20*, 1. (d) Rehm, T. H. *ChemPhotoChem* **2020**, *4*, 235. (e) Di Filippo, M.; Bracken, C.; Baumann, M. *Molecules* **2020**, *25*, 356.
- (12) Ley, S. V.; Chen, Y.; Fitzpatrick, D. E.; May, O. S. *Curr. Opin. Green Sustainable Chem.* **2020**, *25*, 100353.
- (13) Donnelly, K.; Baumann, M. *J. Flow Chem.* **2021**, *11*, 223.
- (14) Ramanathan, M.; Wang, Y.-H.; Liu, S.-T. *Org. Lett.* **2015**, *17*, 5886.
- (15) CCDC 2221466, CCDC 2221467, and CCDC 2221468 contain the supplementary crystallographic data for this paper. These data can be obtained free of charge from The Cambridge Crystallographic Data Centre via www.ccdc.cam.ac.uk/structures
- (16) (a) Bracken, C.; Baumann, M. *J. Org. Chem.* **2020**, *85*, 2607. (b) Donnelly, K.; Baumann, M. *Chem. Commun.* **2021**, *57*, 2871.
- (17) (a) Bracken, C.; Batsanov, A. S.; Baumann, M. *SynOpen* **2021**, *5*, 29. (b) Di Filippo, M.; Baumann, M. *Eur. J. Org. Chem.* **2020**, *2020*, 6199.
- (18) Oligomerisation of the dipolarophile was observed when using the high-power LED emitting at 365 nm.